Available online at www.sciencedirect.com
SCIENCE DIRECT
Atmospheric Environment 40 (2006) 3057–3069
ATMOSPHERIC ENVIRONMENT
www.elsevier.com/locate/atmosenv

Photochemical ozone production in the Eastern Mediterranean

Evangelos Gerasopoulos, Giorgos Kouvarakis, Mihalis Vrekoussis, Christos Donoussis, Nikolaos Mihalopoulos, Maria Kanakidou*

Environmental Chemical Processes Laboratory, Department of Chemistry, University of Crete, P.O. Box 2208, GR71003 Voutes, Heraklion, Greece

Received 9 August 2005; received in revised form 11 December 2005; accepted 15 December 2005

Abstract

A 7 year time series (1997–2004) of surface ozone at Finokalia, Crete, in the Eastern Mediterranean, was analysed to investigate the factors that control the diurnal variability of ozone, and evaluate seasonally distributed ozone production/destruction rates in the area. The observed diurnal evolution of related chemical/physical parameters indicates that ozone morning built-up is driven by photochemistry while during summer the entrainment from the free troposphere is the dominant process in the afternoon. The observed similar behaviour of ozone maxima and Radon-222 minima supports that entrainment from the free troposphere affects the ozone diurnal pattern. Ozone nighttime depletion is mainly attributed to deposition and to a lesser extent to chemical reactions. On an annual basis the role of local photochemistry is found to be limited (-1–$1.7\,\mathrm{ppbv\,d^{-1}}$) contributing by less than 4% to the observed ozone levels. During summer the enhanced ozone destruction via deposition and chemistry are almost balanced by the chemical production and the entrainment of ozone rich air masses from the free troposphere that maximizes in summer (4–6% of the observed ozone levels). Chemical box model simulations also indicate low net chemical production in the area throughout the year that results from high chemical production and destruction terms. Especially during summer photochemical ozone depletion over the area is revealed both by model results and observations (0.5–$1.0\,\mathrm{ppbv\,d^{-1}}$).

Keywords: Ozone photochemical production; Eastern Mediterranean; Marine boundary layer; Diurnal cycle

1. Introduction

Ozone (O_3) has been established as a pollutant (WMO, 1999) with definite impact on humans and ecosystems, and as an important greenhouse gas (e.g., Roelofs et al., 1997). Tropospheric ozone levels are modulated by the amounts of ozone transported from and to the stratosphere in the extratropics and tropics, respectively, as well as by ozone photochemical production in the troposphere. However, the time evolution of ozone concentrations in a tropospheric air parcel is determined by a number of chemical and dynamical processes, namely photochemical production, deposition on surfaces, heterogeneous losses on aerosols, vertical entrainment and horizontal dispersion (Trainer et al., 2000; Monks, 2000). Ozone diurnal variability is mainly driven by the variations of precursor trace gases while the role of local meteorology should not be disregarded (Fischer

*Corresponding author. Tel.: +302810545033; fax: +302810545001.
E-mail address: mariak@chemistry.uoc.gr (M. Kanakidou).

1352-2310/$ - see front matter © 2006 Elsevier Ltd. All rights reserved.
doi:10.1016/j.atmosenv.2005.12.061

et al., 2003). Little information exists concerning the role of aerosols in tropospheric photochemistry, however changes in the aerosol content are expected to affect considerably the photolysis of ozone (Liao et al., 1999; Zanis et al., 2002; Tie et al., 2005) and the rates of heterogeneous losses of ozone and its precursors. Finally, the effect of UVB and stratospheric columnar ozone on the formation of tropospheric ozone is also believed to be important (Zanis et al., 2002).

Recent reviews of ozone production based on observations in rural environments are given by Monks (2000), Kleinman (2000) and Trainer et al. (2000). Both models and observations demonstrate that ozone production is usually nitrogen oxides (NO_x) limited (Fischer et al., 2003). In the presence of sufficient amounts of NO_x the oxidation of carbon monoxide (CO) and volatile organic compounds (VOCs) is a significant source of ozone (Crutzen, 1973; Chameides and Walker, 1973). The quantification of ozone production rates has been under scrutiny over the past decade. Trainer et al. (2000) and Kleinman (2005) refer to different approaches for the calculation of ozone production rates based on either direct measurements of NO and peroxy radicals, or photo-stationary state relations, or photochemical box models. In either case, observational analyses, including accurate measurement of ozone precursors, are important for the correct determination of the net ozone production.

The knowledge of the factors that modulate ozone diurnal variability and its production and destruction rates is essential for environmental policy definition. The Mediterranean is an area of high photochemical activity and a cross-road of air masses of different origin (Lelieveld et al., 2002). Therefore it is considered as a ''hot spot'' area for climate change due to the observed ozone built-up and high aerosol loadings. Gerasopoulos et al. (2005) have recently shown that the most important mechanism controlling ozone interannual and seasonal variability in Crete (Greece) is transport of pollution from the main European continent in agreement with earlier results by Lelieveld et al. (2002) for summer. However, the evaluation of the extent in which the photochemistry determines ozone variability required additional data and further interpretation.

To our knowledge, the studies of ozone production in the Mediterranean are rather limited in number and concern ozone production rates during short campaigns (10–15 days; Zanis et al., 2002; Fischer et al., 2003). The present work attempts to provide insight on the factors that control the diurnal variability of ozone, and to evaluate seasonally distributed ozone production/destruction rates. It is supported both by observations and by chemical box model calculations. The different processes responsible for the ozone built-up and depletion are distinguished and their contributions are quantified.

2. Experimental

Surface ozone measurements are conducted at Finokalia (35°20′N, 25°40′E), the monitoring station of the University of Crete, Greece, during the period 1997–2004. The station is situated 70 km northeast of Heraklion at the northern coast of Crete. A recent description of the site is given by Vrekoussis et al. (2004).

A number of chemical, physical and meteorological ancillary parameters have been also measured. The photo dissociation rates of ozone ($JO\ ^1D$) and nitrogen dioxide (JNO_2) are used as indicators of the intensity of the photochemical activity. The nitrogen oxide (NO) and the reactive nitrogen compounds (NO_z') are deployed as tracers of pollution (either transported or local). NO_z' here expresses mainly the sum of NO_2, NO, peroxyacetyl nitrate (PAN)-like compounds, organic nitrates and nitric acid. Black carbon (BC) is used to detect the influence from burning activities either at the vicinity of the station or after long-range transport. The natural radionuclide radon-222 (Rn) is used as indicator of transport in both the horizontal and the vertical directions. Elevated Rn values are observed in air masses of continental origin (Gerasopoulos et al., 2005) while low Rn concentrations characterize air masses of maritime or free tropospheric origin.

2.1. Instrumentation and methodology

Details on the instrumentation, the time coverage of the measurements and basic statistical information can be found in Kouvarakis et al. (2000), Gerasopoulos et al. (2005). In the present study, continuous measurements of the photo dissociation rates $JO\ ^1D$ and JNO_2 by filter radiometers (Meteorologie Consult, Germany) for the periods July 2000–August 2000 and June 2001–December 2004 are additionally used. The accuracy of these measurements is determined to be 15%, and the

precision better than 3% (see Berresheim et al., 2003). The sensors are calibrated yearly against a spectral radiometer at the Research Center Juelich, Germany (B. Bohn, pers. comm.). NO_z' is experimentally determined by a Thermo Environmental Model 42C high sensitivity chemiluminescence NO_x analyzer equipped with a molybdenum converter that in addition to NO and NO_2, allows detection of PAN, nitric acid, and organic nitrates.

Hourly averages are extracted for all parameters and local time (LT) is used in the manuscript (Local time = UTC +2 and +3 during winter and summer, respectively). Air sampling for Rn activity measurements is conducted on a 2-h basis. For the construction of the hourly time series, Rn activity is assumed to be constant within each 2-h sampling interval.

2.2. Model description

The box model used in this study has been described in Poisson et al. (2001), Tsigaridis and Kanakidou (2002) and Vrekoussis et al. (2004). Observed hourly mean values per season of O_3, CO, NO, JNO_2, JO ^{1}D, temperature, relative humidity (RH) and wind speed are used as input to the chemical box model employed for the present study. NO_2 nighttime values measured by DOAS (Vrekoussis et al., 2006) are also used as input to the model. Isoprene, ethene, propene, ethane, propane and butane mixing ratios were based both on measurements performed in the area during an 8-month period (February–October 2004; Mihalopoulos and Bonsang, unpublished data) and in the western Mediterranean (Plass-Dülmer et al., 1992). No direct heterogeneous ozone losses are included in the model whereas NO_z' and RO_x heterogeneous losses are parameterized as described by Tsigaridis and Kanakidou (2002) and Vrekoussis et al. (2004).

3. Results and discussion

3.1. Data presentation

For the first time 3.5 year measurements of the photo dissociation rates JO ^{1}D and JNO_2 at Finokalia station are presented and used to understand ozone photochemistry. In the past, JO ^{1}D and JNO_2 have been measured in the Eastern Mediterranean during short-term field experiments. In spring (May 1999) during the PAUR campaign, Balis et al. (2002) have measured the photolysis rates of O_3 and NO_2 on Crete. Local noon JO ^{1}D values ranged from $2.4\times10^{-5}\,s^{-1}$ to $3.4\times10^{-5}\,s^{-1}$, whereas JNO_2 ranged from $8\times10^{-3}\,s^{-1}$ to $9.9\times10^{-3}\,s^{-1}$. Summertime measurements at Finokalia during the MINOS campaign (August 2001; Berresheim et al., 2003) show median daytime levels of JO ^{1}D from $0.9\times10^{-5}\,s^{-1}$ to $1.4\times10^{-5}\,s^{-1}$ and of JNO_2 from $6.7\times10^{-3}\,s^{-1}$ to $7.9\times10^{-3}\,s^{-1}$. In the present study, the annual variation of the daytime medians of the measured photo dissociation rates is depicted in Fig. 1 together with that of ozone. JO ^{1}D presents a July maximum of $1.2\times10^{-5}\,s^{-1}$ ($6.8\times10^{-6}\,s^{-1}$ for 24-h averaging) while a more flat pattern is found for JNO_2 with a June maximum of $5.8\times10^{-3}\,s^{-1}$ ($3.6\times10^{-3}\,s^{-1}$ for 24-h averaging). Minima are found in winter and are 5.5 and 4.5 times lower than the maxima for JO ^{1}D and JNO_2, respectively. These patterns are in coincidence with ozone variation pointing to a significant link between photochemistry and the observed ozone variability. In addition, it has been shown that the ozone summer maximum in the area is related with transport from the main European continent (Gerasopoulos et al., 2005). The relative importance of these two processes for ozone variability is investigated further in the present study.

3.2. Diurnal cycles

Fig. 2 presents the mean diurnal cycles of ozone, the photolysis rates of O_3 and NO_2 and chemical/physical parameters. Four characteristic slopes that vary seasonally are observed in the ozone diurnal cycle, as shown in Fig. 2(a). Ozone presents a daily minimum of 46 ± 11 ppbv (34 ± 7 ppbv in December and 54 ± 9 ppbv in August, values after $\pm$ correspond to the standard deviation of the hourly means) at 08:30 (Fig. 2(a)). The daily maximum of ozone is 50 ± 12 ppbv (37 ± 7 ppbv in December and 59 ± 11 ppbv in August) and it is found in the afternoon. Two slopes constitute the descending branch. The first slope (slope 1) is found from the beginning of the night until about 06:30 and expresses ozone nighttime destruction mainly via deposition. After 06:30 when also NO and NO_z' start rising (Fig. 2(b)), the drop of ozone becomes steeper denoting higher destruction of ozone by chemical reactions or enhancement of its loss by deposition (slope 2). On a yearly mean basis, the ascending branch is found from 08:30 to 18:30 in coincidence with the high photochemical activity period of the day as shown by the JO ^{1}D and JNO_2

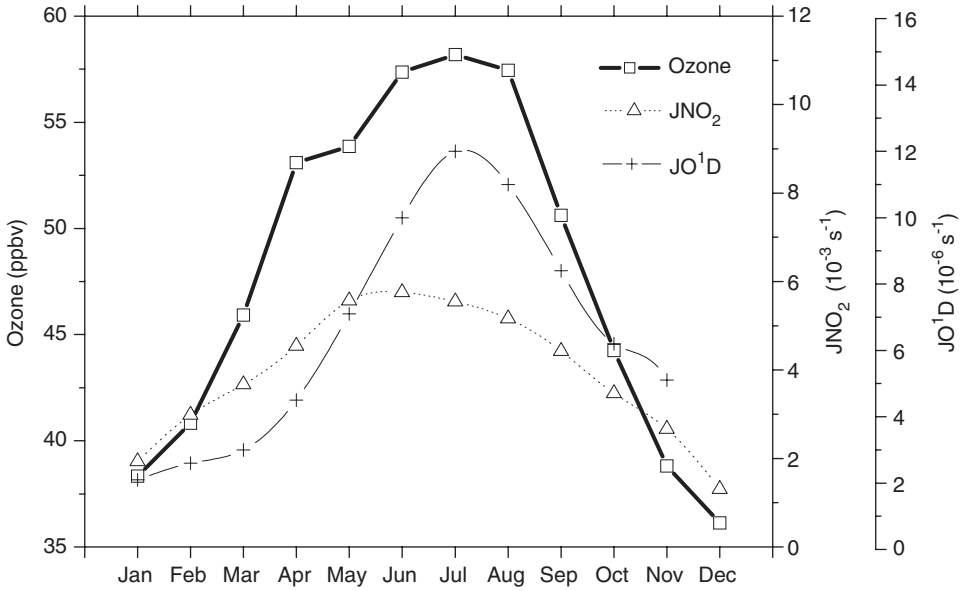

Fig. 1. Annual cycles of ozone and the photolysis rates of O_3 and NO_2. Photolysis rates are daytime medians (6:00–20:00 LT).

values. The rate of ozone built-up seems to be the highest until about 13:00 (slope 3a) (period of increasing photolysis rates) and then weakens progressively until ozone reaches its plateau in late afternoon (slope 3b) when JO ^{1}D and JNO_2 are close to the detection limit of the instruments.

To investigate the factors driving the diurnal variability of ozone, the diurnal cycles of other related physical and chemical parameters measured at Finokalia are also analyzed. NO and NO_z' (Fig. 2(b)) both start rising when photochemistry begins (JO ^{1}D and JNO_2 increase) and their maxima are found 3–4 h later in the morning. Then they are gradually reduced reaching their night levels after 19:00.

The investigation of wind diurnal changes does not support the existence of any systematic sea–land-breeze circulation. Thus, the monthly (and seasonally) mean diurnal patterns discussed here are not expected to be influenced by such occasionally occurring circulation patterns. Rn presents a distinct diurnal variability with maximum values during night/early morning and minimum in the afternoon (Fig. 2(b)), in anti-correlation with ozone. However, the time that Rn maxima and minima are observed strongly depends on season, as discussed further in Section 3.3 and shown in Fig. 3(b). Rn diurnal cycle possibly reflects the changes in the stability of the boundary layer (BL), which enables or prohibits ozone entrainment from the free troposphere. BC shows no significant diurnal variability and this feature is maintained when diurnal cycles are extracted for each month separately. This is possibly related with the fact that emissions from local burning activities are well mixed within the boundary layer thus having no impact on the diurnal variability of BC.

3.3. Seasonal evolution of diurnal cycles

The diurnal cycles described above correspond to the average pattern for all seasons. The month-by-month differences of some specific characteristics of these patterns such as the local time at which maxima, minima and start of daytime rising occur, are presented in Fig. 3. From the seasonal evolution of the diurnal cycles of the various chemical/physical parameters information is deduced on the factors that control the duration or the change in the rates of ozone built-up/depletion.

The diurnal evolution of the photo dissociation rates (JO ^{1}D, JNO_2) reflects the change of the daylight duration. JNO_2 starts rising at 6:30 during spring and summer and at 7:30 during winter and fall (not shown). JO ^{1}D that requires shorter wavelengths than NO_2 photolysis follows an hour later. Their maxima are observed mostly in coincidence, shifting from 11:30 in winter to 13:30 in

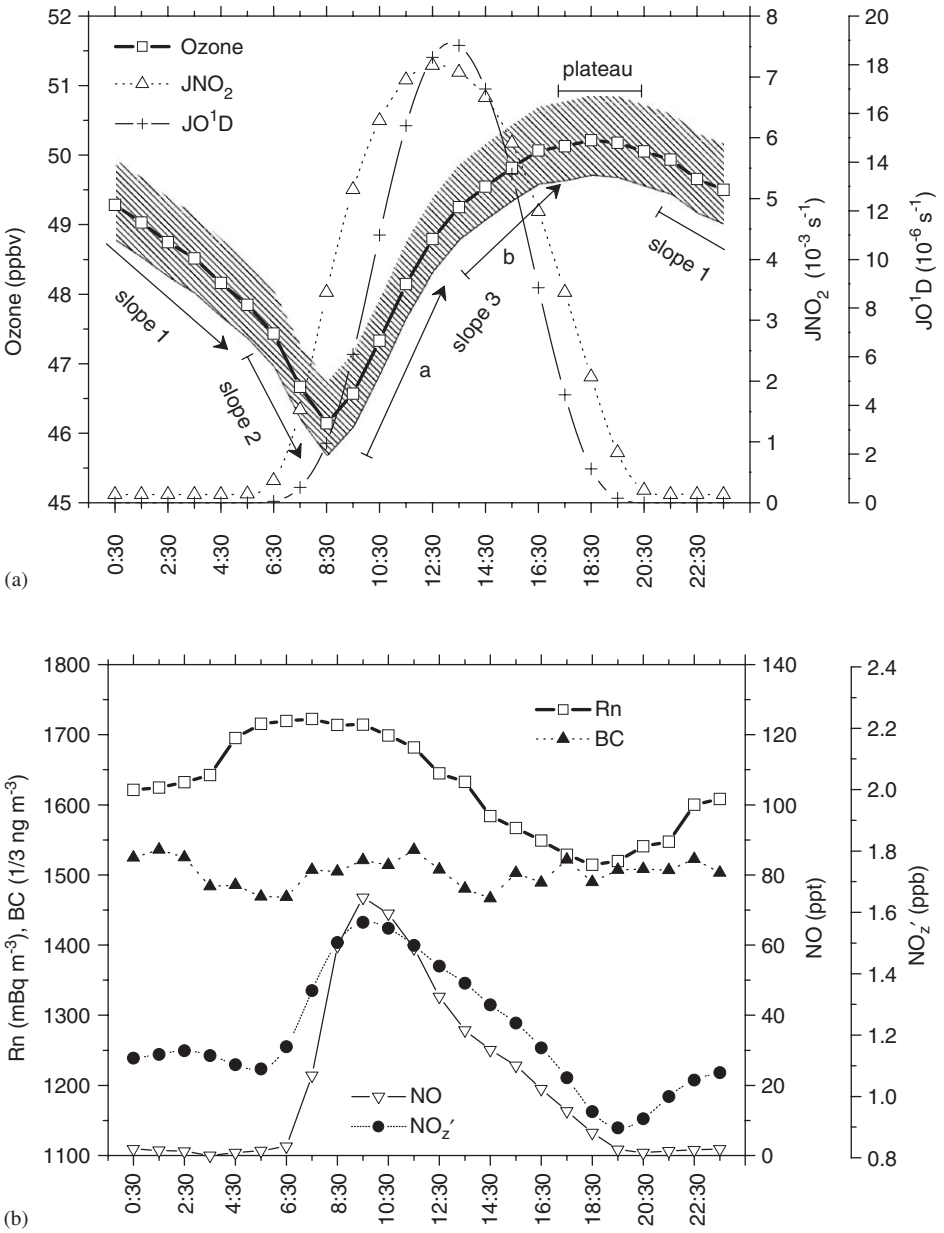

Fig. 2. Diurnal cycles of (a) ozone and the photolysis rates of O_3 and NO_2 (the shaded area corresponds to the 95% confidence level of ozone hourly means), (b) physical (BC, Rn) and chemical (NO, NO_z') parameters.

summer. They reach again the night values around 17:30 in winter and around 21:30 in summer, with JNO_2 lagging 1 h JO ^{1}D so that a broader distribution is revealed for JNO_2 within a day.

Ozone minimum is observed at 08:30 throughout the year, with 1 h delay from the time that NO starts rising (at 07:30, Fig. 3(a)). Most of the year NO_z' starts its morning increase simultaneously with NO except during the warmest months (April–August) when its rise precedes by one hour the NO ascent. In summer, ozone minimum coincides with both NO and NO_z' maxima at 08:30, but in winter and early spring these maxima are shifted toward noon resulting in a longer period of NO and NO_z' built-up.

In winter, ozone maxima are observed between 15:00 and 17:00, while in summer they occur later in the afternoon and early evening (18:00–21:00). This

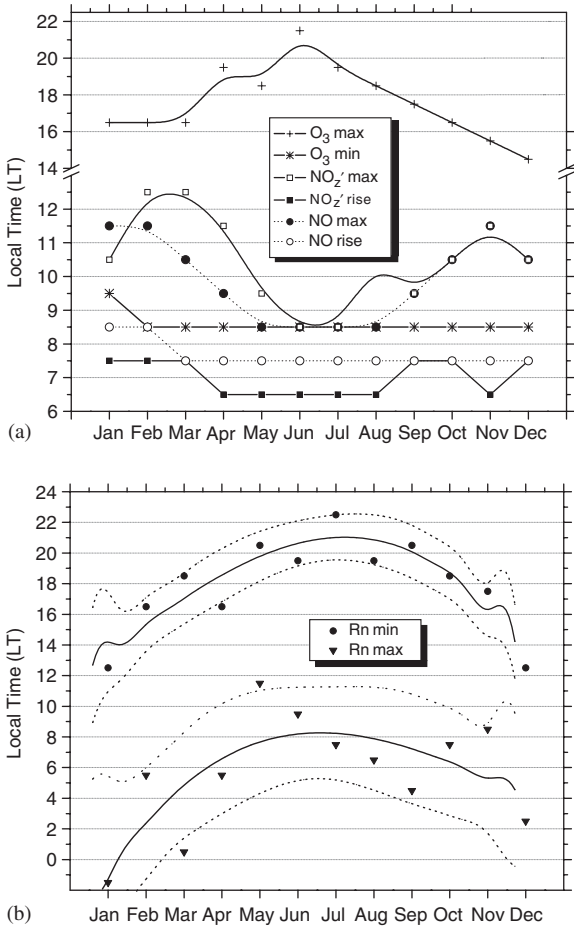

Fig. 3. Local time of the occurrence of maxima, minima and/or start of daytime rising for (a) O_3, NO, NO_z', (b) Rn.

prolongation of ozone built-up period follows that of sunlight (and thus of the photolysis rates) indicating a photochemical origin in the changes of ozone during day. However, ozone maxima seem to tag along with Rn minima that are found around 13:00 in winter and around 21:00 in summer. Taking also into account the role of Rn as an index for the discrimination of the history of air masses arriving at the station, the observed similar behaviour of ozone maxima and Rn minima identifies transport as an additional mechanism affecting the ozone diurnal pattern. Thus, this covariance between ozone and Rn diurnal cycles has been investigated in more detail.

Cross-correlation between ozone and Rn diurnal cycles: The correlation coefficients for linear regression between the mean diurnal cycles of ozone and Rn were calculated for each month separately and are presented in Fig. 4. Additional cross-correlation

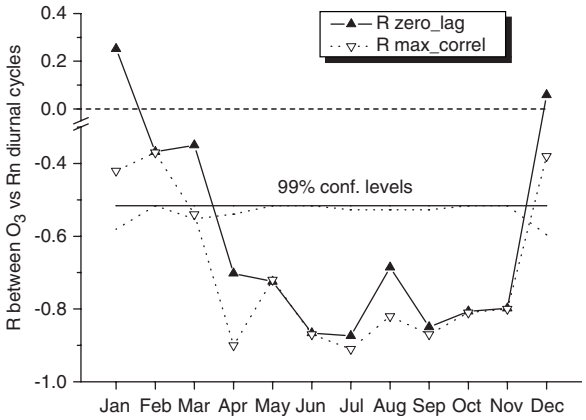

Fig. 4. Correlation coefficients for linear regression between ozone and Rn diurnal cycles for each month (closed triangles) and 99% confidence level (solid line). Maximum cross-correlation coefficients (open triangles), see text, and 99% confidence level (dotted line).

analysis was performed for the calculation of the maximum correlation coefficients after shifting the diurnal cycle of ozone with respect to the corresponding cycle of Rn. In both cases a significant anti-correlation at the 99% confidence level is revealed for the period April–November while in winter this anti-correlation does not occur. The anti-correlation is mainly due to the parallel shift of ozone maximum and Rn minimum to late afternoon towards summer and expresses the entrainment of free tropospheric air rich in ozone and lacking Rn in the BL.

3.4. Amplitude of ozone diurnal cycle

The ozone maximum at Finokalia station that is found in summer (Fig. 1) is mainly attributed to transport of ozone and its precursors from the main European continent and more precisely from NE Europe (Gerasopoulos et al., 2005). In the present study we compare the diurnal maximum with the corresponding minimum to constrain the role of local photochemistry. Thus, the difference between the maximum and the minimum ozone concentration was calculated for each day. Statistical information on the seasonal variability of ozone amplitude is provided via the box-whiskers chart (Fig. 5). Ozone diurnal amplitude ranges between 7 and 12 ppbv with maximum in summer and minimum in winter. On an annual basis, minimum ozone amplitudes are around 2.5 ppbv while a rise of 20–35 ppbv can be encountered in certain cases.

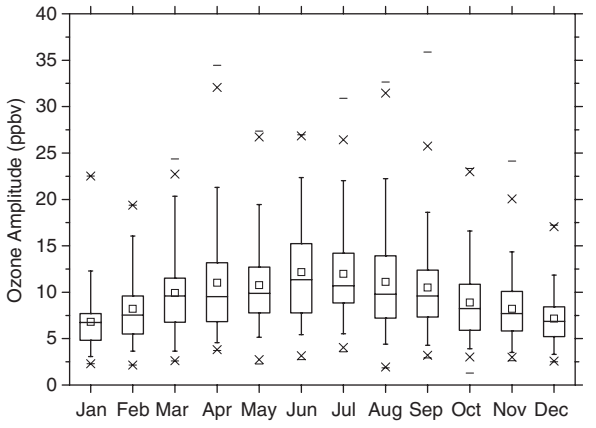

Fig. 5. Amplitude of ozone diurnal cycles per month: The boxes correspond to the upper (75%) and lower quartiles (25%) and the dashes and squares inside the boxes represent the median and the average of the amplitudes, respectively. The error bars attached to the boxes are the 5% and 95% percentiles and the "x" are the 1% and 99% percentiles. The dashes outside the boxes indicate the minimum and maximum amplitudes, respectively.

When ozone amplitude is divided by the mean value of the corresponding month then no particular pattern is revealed (averaged ratio $20\pm1\%$) and only in January a drop to 17.4% is found. Thus, throughout the year similar ozone percent change is encountered and the observed seasonal differences in ozone amplitude could be attributed to changes in ozone levels.

4. Ozone changes derived from observations and model calculations

4.1. Observed rates of ozone built-up and depletion

For each monthly mean diurnal cycle of ozone, the rates of ozone built-up and depletion are estimated as slopes of consecutive points. The four slopes shown in Fig. 2(a) are calculated and presented in Fig. 6(a) as a function of the month. All calculated slopes present high squared correlation (R^2), significant at the 99% confidence level.

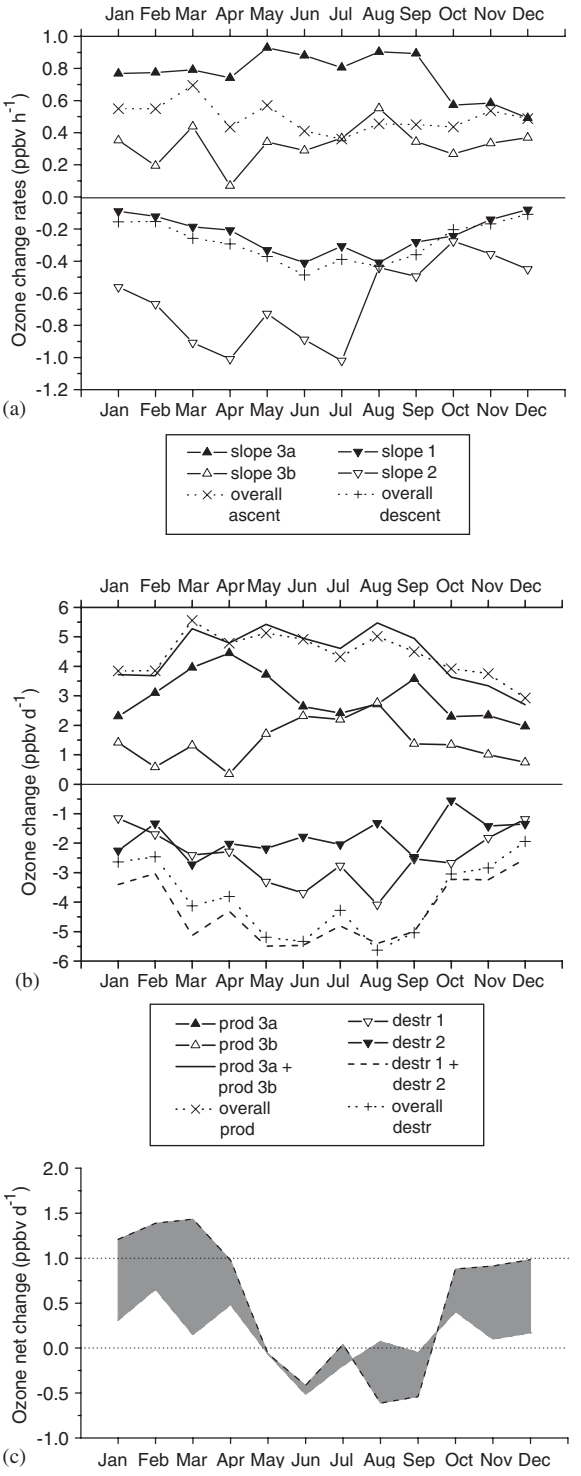

Fig. 6. (a) Seasonal variation of ozone built-up (positive) and depletion (negative) rates corresponding to the slopes shown in Fig. 2(a). An overall slope for each branch is also presented, (b) seasonal variation of ozone production (positive) and destruction (negative) calculated as the product of each slope and the corresponding duration. The sum of the productions/destructions from the individual slopes (prod 3a + prod 3b, destr 1 + destr 2) is presented together with the overall production/destruction when one slope is considered for each branch (overall prod/destr), (c) the shaded area corresponds to the net ozone production as the sum of production and destruction terms for each approach (the dashed border of the area represents the values from the overall slope approach).

Additionally, the BL height derived from radiosoundings does not show strong seasonal variability, allowing the direct comparison of the ozone change rates issued from surface observations, on a seasonal basis. In particular, monthly mean BL heights ranged between 1000 and 1300 m and the use of the *t*-Student's test proved that the difference between summer and winter values is not significant at the 99% confidence level.

The rate of nighttime ozone destruction that is attributed mainly to deposition (slope 1) is higher in summer (0.4 ppbv h^{-1}) and decreases in winter (by a factor of 5), as expected because the deposition depends on ozone concentration (e.g. Wesely and Hicks, 2000) that is 1.6 times lower during winter. In particular, a significant at the 99% confidence level correlation between ozone monthly mean concentrations and slope 1 is found ($R^2 = 0.84$), corresponding to a mean deposition velocity of 0.15 cm s^{-1} for a BL height of 1200 m. This deposition velocity is higher than the reported velocities over oceans, 0.01–0.05 cm s^{-1}, but still significantly lower than the deposition over agricultural land (e.g. Wesely and Hicks, 2000) and also includes nighttime ozone destruction by alkenes and NO_2. Early in the morning, with NO and NO_z' present (slope 2), the rate of ozone destruction increases and maximizes between March and July (0.7–1 ppbv h^{-1}) while this rate is drastically weakened after August (0.3–0.5 ppbv h^{-1}). During winter and spring (December–April) the early morning ozone destruction is enhanced by 0.09 ppbv O_3 h^{-1} per ppbv NO ($R^2 = 0.92$), while in summer this relation is masked due to the enhanced contribution of deposition to slope 2 or to the potential involvement of halogen chemistry as will be further discussed. Therefore, for the period August–November the two slopes (slopes 1 and 2) do not differ considerably, whereas their discrimination is evident in winter and spring.

In winter, the daytime increase of ozone concentrations is more uniform until the maximum is reached whereas in spring and summer a secondary slope is observed (Fig. 2(a), slope 3b). The rate of ozone increase (slope 3a) appears slightly higher from May to September (around 0.9 ppbv h^{-1}) than from October through December (0.6 ppbv h^{-1}) and from January through April (0.8 ppbv h^{-1}) (Fig. 6(a)). A linear relation between monthly mean JNO_2 and slope 3a is found from March to December ($R^2 = 0.78$). No particular relation is observed between slope 3b and any of the parameters.

The mean duration of each slope is also important for the impact of the associated process on the ozone change per day. The nighttime deposition in summer (slope 1, Fig. 2(a)), even though more intense, lasts about 9 h (not shown here) whereas in winter and spring its duration ranges between 13 and 15 h linked to the length of the day and the shift of ozone maximum from noon in winter to late afternoon in summer. No particular seasonality is observed for the duration of slope 2 (early morning decrease in ozone) and slope 3a (late morning increase in ozone). The last is almost constant with season with a slight enhancement in spring. Finally, the duration of slope 3b maximizes in summer mainly as a consequence of the increase in the length of the day.

The ozone change, calculated as the product of the slopes and the duration of their occurrence, carries enhanced uncertainty after error propagation. Therefore, slopes are also calculated for the overall descending, slope (1 + 2), and the overall ascending, slope (3a + 3b), branches, respectively (dotted lines in Fig. 6(a and b)), that are associated with smaller uncertainty in the duration than the individual slopes even though the linearity is worse.

For each month, combining the slopes with their duration, a first estimation of the seasonal variability of ozone built-up and depletion is derived (Fig. 6(b)). The nighttime destruction linked to slope 1 presents a summer maximum of about 4 ppbv d^{-1} and dominates over the early morning destruction (slope 2) during the warmest period. From September through April the early morning destruction has an equal contribution to daily ozone budget as the nighttime destruction regardless of its much shorter duration. Year-round the total ozone destruction per day ranges between 2 and 5.5 ppbv with a broad spring–summer maximum. When the destruction is calculated from the overall descending slope (associated with smaller uncertainty than the individual ones) instead of the sum derived from slopes 1 and 2, the same pattern is revealed and the two results agree within less than 23%. Concerning the ascending ozone branch, morning ozone built-up (slope 3a) is in general dominant over the afternoon increase, slope 3b, with a spring peak of 4.5 ppbv d^{-1}. The ozone gain linked to the afternoon increase (slope 3b) peaks in summer and is of the same importance as the morning ozone built-up during that season. When the production is calculated from the overall ascending slope, the

same spring–summer maximum is revealed and the two results agree within less than 12%.

To obtain the net ozone change the difference between ozone production and destruction is calculated both with the individual slopes and the overall slope approaches (Fig. 6(c)). On a yearly basis, the first approach (individual slopes) provides a net ozone change of 0.13 ± 0.32 ppbv d^{-1} while a value of 0.52 ± 0.78 ppbv d^{-1} is derived from the second approach (overall slope). Both results indicate small rates of ozone change. Even though the uncertainty in these estimations is high, they indicate clearly that the ozone change rates are low while their seasonality should be regarded with caution. However, the low winter ozone gain found with both approaches (0.3–1.5 ppbv d^{-1}) is possibly associated with regional photochemical production favoured by the enhanced insolation in southern Greece compared with northern areas from where ozone precursors originate. On the other hand, during summer low ozone destruction (up to 0.5 ppbv d^{-1}) is encountered over the area. The low rates calculated for summer possibly reflect the fact that the photochemical aging of ozone precursors is accomplished over the main European continent or that enhanced ozone destruction almost counterbalances the ozone built-up in the area.

4.2. Comparison between observations and model

A chemical box model has been used to analyse the observations and identify the major chemical processes involved in ozone production and destruction. To compare with the model results another approach of calculating the observed ozone built-up and depletion rates is needed that additionally provides the diurnal evolution of the rates that is not retrieved by the earlier presented slope approach. Therefore, slopes of N ($N = 2, 3, 5$) consecutive points (hours) are calculated from the hourly time series of ozone at Finokalia. The starting point is shifted by 1 h every time and each slope is attributed to the mid hour of the N points. The derived slopes correspond to the rate of ozone change at this particular hour and the mean diurnal patterns of ozone rates are calculated for each month and for each season. Increasing N smoothes the derived patterns, without nevertheless, changing the characteristics of the diurnal evolution or the net surface beneath the lines. The 5-point moving slopes will be used henceforth. The diurnal evolution of the rates of ozone change derived from the observations (5-point moving slope approach) is extracted for each month (not shown). The mean seasonal patterns of these rates together with the chemical box model results are presented in Fig. 7.

A relatively good agreement between model and observations is found in all seasons except summer. In particular, the model results show lower production rates than the observations in winter (still both indicate low production rates), while during fall the peak rates are well simulated and during spring the observed patterns appear broader towards evening peaks. Nighttime destruction is well simulated on an annual basis but the enhanced destruction in early morning made apparent from the observations is not captured by the model which presents such a feature only in summer. The highest discrepancy between model and observations is found in summer when observed rates do not exceed 0.72 ppbv h^{-1}, while rates derived from the model rise up to 0.5 ppbv h^{-1} in the morning. A destruction rate is calculated for the afternoon mainly due to enhanced chemical ozone depletion as explained below.

According to our model calculations this net chemical ozone production is the result of a large ozone chemical production $P(O_3)$ and a large ozone chemical destruction $L(O_3)$ (Fig. 8). The $P(O_3)$ is driven by the reaction of hydrogen and organic peroxy radicals ($HO_2 + RO_2 = RO_x$) with NO and on a seasonal mean basis varies from about 2.6 ppbv d^{-1} in winter to about 5.6 ppbv d^{-1} in summer. Note that the model simulated RO_x levels are in good agreement with the seasonally mean observations in the area (unpublished data), thus confirming the modelled $P(O_3)$ terms. The $L(O_3)$ maximises in summer reaching about 6.6 ppbv d^{-1} and goes down to 1.2 ppbv d^{-1} in winter when photochemical activity and water vapour are low. Indeed, as mentioned above the ozone chemical loss is mainly driven by reaction of $O\ ^1D$ with water vapour that also maximises in summer. This reaction contributes to the $L(O_3)$ by more than 25% year-round and by 3.8 ppbv d^{-1} that is about 58% during summer. By far the second more important ozone chemical loss process is the catalytic cycle of OH/HO_2 (up to 2.3 ppbv d^{-1}) that also follows the same seasonal pattern with the $L(O_3)$. Its contribution to $L(O_3)$ is between 35% and 42% with the minimum contribution in winter and the maximum in spring.

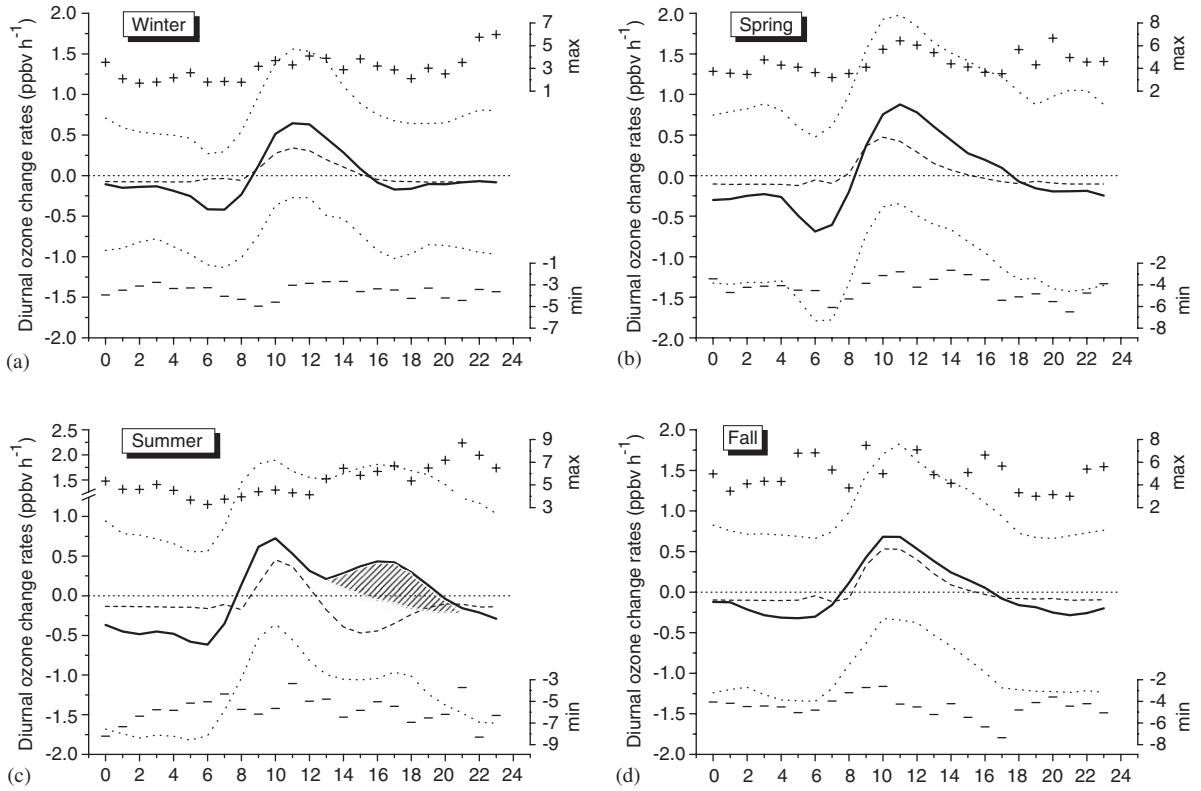

Fig. 7. Diurnal variation of ozone change rates derived both by model (dashed line) and observations (solid line: averages, dotted lines: standard deviation, (+)/(−): maximum and minimum, see text) for (a) winter, (b) spring, (c) summer and (d) fall. The shaded area in panel (c) is attributed to the contribution of entrainment from the free troposphere.

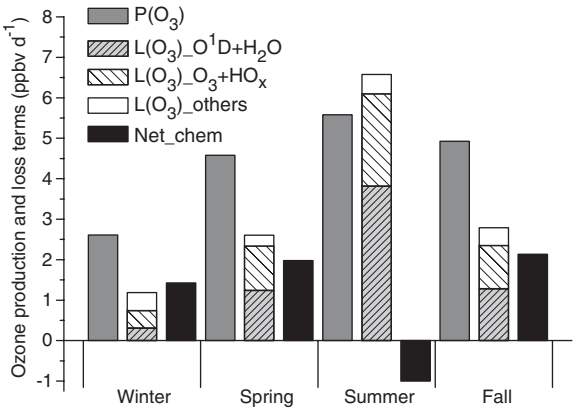

Fig. 8. Ozone production, loss terms and net chemical change (P(O3)–L(O3)) as calculated by the model for the different seasons.

An additional ozone destruction mechanism that has not been included in the model is the reactions with halogens. However, the major halogens deficit in sea-salt aerosol with regard to the sea water composition observed at Finokalia (Kouvarakis, 2002) indicates the release of halogens in the gas phase (Platt and Hönninger, 2003; Sander et al., 2003) and subsequently the potential of halogen chemistry occurrence in the studied coastal environment. As pointed out by von Glasow et al. (2002) and Dickerson et al. (1999) this mechanism could be the reason for sunrise ozone destruction that is revealed by our observations and is not simulated by the model. The model calculates a weaker early morning ozone loss via the reaction with NO that is delayed compared with observations.

Another interesting feature in the diurnal evolution of ozone change from observations is a bimodal pattern resulting from a secondary "hump" on the descending branch of ozone production found between April and September. This is shown as a shaded area in the summer diurnal pattern (Fig. 7(c)). The secondary peak in the rates of ozone change occurs between 17:00 and 18:00 from April

to June and at 16:00 from July to August. The parallel shift of ozone diurnal maxima and Rn diurnal minima during summer indicates that a non-chemical mechanism may be responsible for this second ozone built-up possibly involving entrainment from the free troposphere, without nevertheless excluding that part of this enhancement might be due to late ozone chemical production.

In the following this second daytime peak in ozone during summer has been investigated inter-annually for the whole studied period (1998–2004). Whether this second and henceforth called "entrainment" peak is clearly distinguished from the photochemical peak of ozone built-up or not, depends on the time difference of the occurrence of the two peaks. When the entrainment peak is close to ozone photochemical morning peak, it is hardly separated and the confidence that a different process is the reason for the secondary peak is lower. Under this scope, a pronounced summer entrainment peak is observed in all years except in 1999 and in 2003. With the exception of these 2 years the coincidence of the entrainment peak with the Rn minimum is remarkable, strengthening our point on the origin of the secondary peak. The most exceptional year as for the intensity of the entrainment is found to be 2004. During this year the entrainment peak is 1.5 times higher than the earlier occurring ozone photochemical peak and is observed at the end of the day around 18:00. To evaluate the overall contribution of the entrainment on ozone changes an exponential decay line has been fitted to the descending branch of the diurnal ozone change rates for each year. The integral between this fitted line and the secondary peak has been attributed to the overall effect of the entrainment on ozone levels (shaded area in Fig. 7(c)). During the period 1998–2004 the mean summertime contribution of entrainment ranged between 0.5 and 3.4 ppbv d^{-1} (2.2 ± 1.0 ppbv d^{-1}) and peaked in 2001 and 2004.

However, the fact that the chemical box model forced by NO observations is not simulating such a secondary peak in ozone additionally supports that a physical process (entrainment) may be at the origin of this ozone peak. In addition to the direct effect on ozone boundary layer levels, the penetration of the free tropospheric air in the boundary layer might result in drier air with higher NO_y levels, therefore inducing late afternoon ozone built-up. This process cannot be simulated by the model based on the available experimental data. These results impose the need for additional observations of the microphysical state of the BL atmosphere together with the chemical parameters to finally conclude on the origin of this secondary peak in ozone.

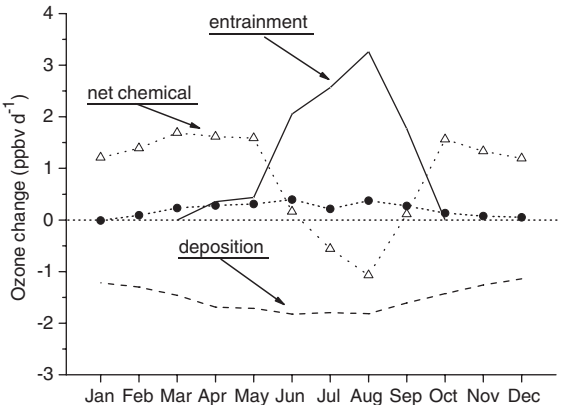

Fig. 9. Ozone change, $D(O_3)/dt$ (closed circles), and its various components namely deposition (dashed line), entrainment (solid line) and the net chemical change (open triangles).

5. Components of ozone change

Integrating the area between the 5-point moving slope cycles and the zero line for each month the net ozone change per day is calculated (Fig. 9). A small net ozone change throughout the year (<0.5 ppbv d^{-1}) is found. This is coherent with the results from the individual and overall slopes approaches (Fig. 6(c)).

The seasonal variability of the various components of ozone change is presented in Fig. 9. The overall effect of entrainment is calculated as described in Section 4.2 on a monthly basis from April through September when the secondary peak was present. It presents a distinct summer maximum contributing 2–3 ppbv of ozone per day that equals 6% of the observed ozone. To exclude any nighttime chemical loss of ozone, deposition has been calculated by the model using a deposition velocity of 0.05 cm s^{-1} and is found to range between -1.1 ppbv d^{-1} in winter and -1.8 ppbv d^{-1} in summer. Subtracting the contribution of both entrainment and deposition from the observed ozone change rates (from the 5-point moving slope approach) the net chemical ozone change is calculated (Fig. 9). This net chemical ozone change presents a minimum of -1.1 ppbv d^{-1} in August (ozone destruction, -0.3 ± 0.6 ppbv d^{-1}, mean from

June through September) whereas during the colder period (October–May) it is 1.4 ± 0.2 ppbv d^{-1}. It contributes by 3–4% to the observed ozone levels from October towards May while during the warmest period ozone destruction up to 2% of the observed ozone levels is encountered.

The results presented here concur with earlier studies over shorter periods. In particular, Zanis et al. (2002) have reported a net ozone production of 0.8 and 1.3 ppbv h^{-1} derived from observations between 06:00 and 12:00 UT on 10 and 20 May 1999 at Nopigia, Crete. The corresponding mean production rate deduced from our observations at Finokalia for May and the same time interval is 0.5 ± 0.2 ppbv h^{-1}, very close to the lower limit reported by Zanis et al. (2002). On 20 May 1999 for which ozone data at Finokalia are available, the calculated mean production rate is 1.4 ± 0.1 ppbv h^{-1} in excellent agreement with the value reported by Zanis et al. (2002). The net ozone production rates at Mt. Cimone (Italy) during the second half of June 2000 has been evaluated by Fischer et al. (2003) to be 0.1–0.3 ppbv h^{-1} (daytime values, 06:00–20:00 UT). These results fit well with our observations of 0.3 ± 0.6 ppbv h^{-1} for the second half of June 2000 and is similar to the mean value of 0.3 ± 0.3 ppbv h^{-1} deduced for the same daytime interval in June and for all years. Note that the standard deviation for the second half of June 2000 refers to the day-by-day variance while that of the overall June pattern refers to the variability of the 06:00–20:00 UT rates. Similar ozone tendencies have been also reported by Salisbury et al. (2002) for summer (0.3 ± 0.1 ppbv h^{-1}) and spring (1.0 ± 0.5 ppbv h^{-1}) at the coastal site of Mace Head (Ireland).

6. Conclusions

This study complements the earlier work by Gerasopoulos et al. (2005) that focused on the physical processes that control ozone's interannual variability and annual maximum values. The present analysis shows that:

- Throughout the year the role of local photochemistry is limited. The ozone net chemical change (-1–1.7 ppbv d^{-1}) contributes by less than 4% on an annual basis to the observed ozone levels either as production or destruction depending on season. Particularly in summer, transport from the main European continent is the dominant mechanism responsible for the elevated ozone in agreement with earlier data analysis by Gerasopoulos et al. (2005), whereas local photochemistry acts as a sink for ozone as revealed both by observations and model.
- On a seasonally mean basis, the diurnal net ozone change is very small (0.2 ± 0.1 ppbv d^{-1}). During summer the enhanced ozone destruction via deposition and the enhanced ozone chemical depletion mainly by the reaction of $O\ ^1D$ with H_2O are almost balanced by chemical production and the entrainment of ozone rich air masses from the free troposphere. This result is further supported by Radon-222 measurements.

Additional observations of the microphysical and chemical state of the boundary layer are needed to conclude on the importance of entrainment on ozone budget and on the role of photochemistry (including halogens) as a source or a sink of ozone in the area during summer.

Acknowledgements

We thank V. Kazan (LSCE) for Radon measurements and PYTHAGORAS II for financial support. EG acknowledges the Greek State Scholarship Foundation for support.

References

Balis, D.S., Zerefos, C.S., Kourtidis, K., Bais, A.F., Hofzumahaus, A., Kraus, A., Schmitt, R., Blumthaler, M., Gobbi, G.P., 2002. Measurements and modeling of photolysis rates during the photochemical activity and ultraviolet radiation (PAUR) II campaign. Journal of Geophysical Research 107 (D18), 8138.

Berresheim, H., Plass-Dülmer, C., Elste, T., Mihalopoulos, N., Rohrer, F., 2003. OH in the coastial boundary layer of crete during MINOS: measurements and relationship with ozone photolysis. Atmospheric Chemistry and Physics 3, 639–649.

Chameides, W., Walker, J.C.G., 1973. A photochemical theory of tropospheric ozone. Journal of Geophysical Research 78, 8751–8760.

Crutzen, P.J., 1973. A discussion of the chemistry of some minor constituents in the stratosphere and troposphere. Pure and Applied Geophysics 106, 1385–1399.

Dickerson, R.R., Rhoads, K., Carsey, T., Oltmans, S., Burrows, J., Crutzen, P.J., 1999. Ozone in the remote marine boundary layer: a possible role for halogens. Journal of Geophysical Research 104, 21385–21395.

Fischer, H., Kormann, R., Klüpfel, T., Gurk, Ch., Königstedt, R., Parchatka, U., Mühle, J., Rhee, T.S., Brenninkmeijer, C.A.M., Bonasoni, P., Stohl, A., 2003. Ozone production and trace gas correlations during the June 2000 MINATROC

intensive measurement campaign at Mt. Cimone. Atmospheric Chemistry and Physics 3, 725–738.

Gerasopoulos, E., Kouvarakis, G., Vrekoussis, M., Kanakidou, M., Mihalopoulos, N., 2005. Ozone variability in the marine boundary layer of the Eastern Mediterranean based on 7-year observations. Journal of Geophysical Research 110, D15309.

Kleinman, L.I., 2000. Ozone process insights from field experiments—part II: observation-based analysis for ozone production. Atmospheric Environment 34, 2023–2033.

Kleinman, L.I., 2005. The dependence of tropospheric ozone production rate on ozone precursors. Atmospheric Environment 39, 575–586.

Kouvarakis, G., 2002. Tropospheric ozone and aerosols over the Eastern Mediterranean. Ph.D. Thesis, Chemistry Department, University of Crete, Greece.

Kouvarakis, G., Tsigaridis, K., Kanakidou, M., Mihalopoulos, N., 2000. Temporal variations of surface background ozone over Crete Island in the South-East Mediterranean. Journal of Geophysical Research 105, 4399–4410.

Lelieveld, J., Berresheim, H., et al., 2002. Global air pollution crossroads over the Mediterranean. Science 298, 794–799.

Liao, H., Yung, Y.L., Seinfeld, J.H., 1999. Effects of aerosols on tropospheric photolysis rates in clear and cloudy atmospheres. Journal of Geophysical Research 104, 23697–23707.

Monks, P.S., 2000. A review of the observations and origins of the spring ozone maximum. Atmospheric Environment 34, 3545–3561.

Plass-Dülmer, C., Ratte, M., Koppmann, R., Rudolph, J., 1992. C2-C9 Hydrocarbons in the Marine atmosphere during NATAC 91. In: Paper Presented at the NATAC 91 Workshop, Odessa, Ukraine.

Platt, U., Hönninger, G., 2003. The role of halogen species in the troposphere. Chemosphere 52 (2), 325–338.

Poisson, N., Kanakidou, M., et al., 2001. The impact of natural non methane hydrocarbon oxidation on the free radical and ozone budgets above a Eucalyptus forest. Chemosphere, Global Change Science 3, 353–366.

Roelofs, G.J., Lelieveld, J., van Dorland, R., 1997. A three-dimensional chemistry/general circulation model simulation of anthropogenically derived ozone in the troposphere and its radiative climatic forcing. Journal of Geophysical Research 102D (19), 23389–23401.

Salisbury, G., Monks, P.S., Bauguitte, S., Bandy, B.J., Penkett, S.A., 2002. A seasonal comparison of the ozone photochemistry in clean and polluted air masses at Mace Head, Ireland. Journal of Atmospheric Chemistry 41, 163–187.

Sander, R., Keene, W.C., et al., 2003. Inorganic bromine in the marine boundary layer: a critical review. Atmospheric Chemistry and Physics 3, 1301–1336.

Tie, X., Madronich, S., Walters, S., Edwards, D.P., Ginoux, P., Mahowald, N., Zhang, R., Lou, C., Brasseur, G., 2005. Assessment of the global impact of aerosols on tropospheric oxidants. Journal of Geophysical Research 110, D03204.

Trainer, M., Parrish, D.D., Goldan, P.D., Roberts, J., Fehsenfeld, F.C., 2000. Review of observation-based analysis of the regional factors influencing ozone concentrations. Atmospheric Environonment 34, 2045–2061.

Tsigaridis, K., Kanakidou, M., 2002. Importance of volatile organic compounds photochemistry over a forested area in Central Greece. Atmospheric Environonment 36 (19), 3137–3146.

von Glasow, R., Sander, R., Bott, A., Crutzen, P.J., 2002. Modeling halogen chemistry in the marine boundary layer–1. Cloud-free MBL. Journal of Geophysical Research–Atmospheres 107 (D17) art. no. 4341.

Vrekoussis, M., Kanakidou, M., Mihalopoulos, N., Crutzen, P.J., Lelieveld, J., Perner, D., Berresheim, H., Baboukas, E., 2004. Role of the NO_3 radicals in oxidation processes in the eastern Mediterranean troposphere during the MINOS campaign. Atmospheric Chemistry and Physics 4, 169–182.

Vrekoussis, M., Liakakou, E., Mihalopoulos, N., Kanakidou, M., Crutzen, P.J., Lelieveld, J., 2006. Formation of HNO_3 and NO_3^- in the anthropogenically-influenced eastern Mediterranean marine boundary layer. Geophysical Research Letters, doi:10.1029/2005GL025069, in press.

Wesely, M.L., Hicks, B.B., 2000. A review of the current status of knowledge on dry deposition. Atmospheric Environment 34, 2261–2282.

WMO, 1999. World Meteorological Organization, Scientific Assessment of Ozone Depletion: 1998, in Global Ozone Research and Monitoring Project Report, Rep. 44, Geneva, ISBN:92-807-1722-7.

Zanis, P., Kourtidis, K., Rappenglueck, B., Zerefos, C., Melas, D., Balis, D., Schmitt, R., Rapsomanikis, S., Fabian, P., 2002. A case study on the possible link between surface ozone photochemistry and total ozone column during the PAUR II experiment at crete: comparison of observations with box model calculations. Journal of Geophysical Research 107 (D18), 8136.